

Accepted Manuscript

Synthesis, characterization and antimicrobial properties of some mixed ligand complexes of Zn(II) dithiocarbamate with different N-donor ligands

Damian C. Onwudiwe, Yvonne B. Nthwane, Anthony C. Ekennia, Eric Hosten

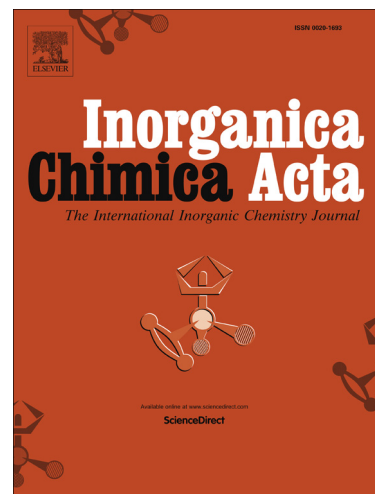
PII: S0020-1693(16)30136-0
DOI: <http://dx.doi.org/10.1016/j.ica.2016.03.033>
Reference: ICA 16968

To appear in: *Inorganica Chimica Acta*

Received Date: 18 February 2016
Revised Date: 23 March 2016
Accepted Date: 24 March 2016

Please cite this article as: D.C. Onwudiwe, Y.B. Nthwane, A.C. Ekennia, E. Hosten, Synthesis, characterization and antimicrobial properties of some mixed ligand complexes of Zn(II) dithiocarbamate with different N-donor ligands, *Inorganica Chimica Acta* (2016), doi: <http://dx.doi.org/10.1016/j.ica.2016.03.033>

This is a PDF file of an unedited manuscript that has been accepted for publication. As a service to our customers we are providing this early version of the manuscript. The manuscript will undergo copyediting, typesetting, and review of the resulting proof before it is published in its final form. Please note that during the production process errors may be discovered which could affect the content, and all legal disclaimers that apply to the journal pertain.



**Synthesis, characterization and antimicrobial properties of some mixed
ligand complexes of Zn(II) dithiocarbamate with different N-donor ligands**

Damian C. Onwudiwe^{1,2*}, Yvonne B. Nthwane^{1,2}, Anthony C. Ekennia³, Eric Hosten⁴

¹Material Science Innovation and Modelling (MaSIM) Research Focus Area, Faculty of Agriculture, Science and Technology, North-West University (Mafikeng Campus), Private Bag X2046, Mmabatho, South-Africa.

²Department of Chemistry, School of Mathematical and Physical Sciences Faculty of Agriculture, Science and Technology, North-West University (Mafikeng Campus), Private Bag X2046, Mmabatho 2735, South Africa.

³Department of Chemistry, Federal University Ndufu-Alike Ikwo (FUNAI), P.M.B 1010, Abakaliki, Ebonyi State, Nigeria.

⁴Department of Chemistry, Nelson Mandela Metropolitan University, P.O Box 77000, Port Elizabeth 6031, South Africa

* Corresponding author

Email: Damian.Onwudiwe@nwu.ac.za

Tel: +27 18 389 2545

Fax: +27 18 389-2420

Abstract

In this study, adducts of Zn(II) dithiocarbamates containing different N-donor ligands (pyridine, 2,2'-bipyridine and 1,10-phenanthroline) have been synthesized. The parent dithiocarbamate complex comprise *N*-methyl-*N*-phenyl dithiocarbamate (L^1) and *N*-ethyl-*N*-phenyl dithiocarbamate (L^2), and the adducts are represented as $[ZnL^1L^2py]$, $[ZnL^1L^2bpy]$, and $[ZnL^1L^2phen]$ (where py = pyridine, bpy = 2, 2'-bipyridine, and phen = 1, 10-phenanthroline). All the compounds have been characterized by elemental analysis and spectroscopic techniques (IR and NMR). In addition, the crystal structure of $[ZnL^1L^2bpy]$ complex is also reported. The structure indicates that the two dithiocarbamate ligands are disordered in 0.67:0.33 ratio and alternatively bond as monodentate and bidentate ligands. The bipyridine acts as a bidentate ligand, and gives the structure around the Zn atom a distorted square pyramidal geometry. In order to evaluate their antimicrobial properties, the precursor complex and the adducts were screened against six pathogenic bacteria strains and two fungi organisms. The antimicrobial activities of the complexes were in the order $[ZnL^1L^2] > [ZnL^1L^2py] > [ZnL^1L^2bpy] > [ZnL^1L^2phen]$. The precursor complex, ZnL^1L^2 , showed the lowest MIC and is considered as the complex with most antimicrobial activity against the selected microorganisms.

Keywords: Zn(II); adducts; X-ray crystal structure; antimicrobial properties.

1. Introduction

The coordination chemistry of zinc is a subject of current interest due to the increasing number of hydrolytic enzymes and DNA binding proteins with Zn(II) in their active sites [1-3]. The biologically active zinc sites are capable of forming adducts with N, O donor ligands, executing efficient and kinetically rapid catalytic reactions due to their variability and flexibility in coordination behaviour [4]. Various synthesized Zinc based compounds have been reported and were used as potent antibacterial, antifungal, anticancer drugs and also as imaging agents [5, 6]. One of such compounds is Zinc dithiocarbamate which shows interesting variations in their reactions with Lewis bases such as phosphines and hard bases like nitrogenous ligands. The possibility of this reaction is due to the unsaturated coordination around the zinc atom in the dithiocarbamate complex, leading to the formation of compounds of higher coordination number either by the addition of one or two molecules of a Lewis base or by dimerization of the Zn dithiocarbamate [7]. The exact nature and reaction mechanism of these adducts is still not fully understood despite several spectroscopic and crystallographic investigations of these compounds. This has prompted several recent studies aiming to understand the structural features of zinc adducts with biologically relevant ligands as synthetic analogues [1, 3].

Dithiocarbamate (DTC) group has been found in a number of biologically active molecules as a pharmacophore [8, 9]. Compounds of dithiocarbamates possess diverse chemical and medicinal versatility. The first dithiocarbamate compound to attain prominence as an antifungal drug was tetramethylthiuram disulfide, commonly known as thiram [10]. Another analogue, Tetraethylthiuram disulfide better known as disulfiram, has been used in the treatment of alcoholism for more than 50 years [11]. Dithiocarbamates have been used as

pesticide and fungicide since 20th century, but have also been of interest to medicinal chemists due to the strongly nucleophilic character and the unique redox properties of the sulfur atom which make it a key residue for enzyme catalysis, protein folding, and redox signaling and regulation. Owing to their strong metal-binding capacity, they can also act as enzyme inhibitors [12].

Adduct formation allow for the increase in coordination number of metal ions in a complex, while maintaining the same oxidation state [13 – 15]. Often, the chemical and biological properties of the resulting adducts are entirely different from their precursor metal complexes [16 – 18]. In order to study the effect of various *N*-donor atoms (pyridine, 2,2'-bipyridine and 1,10-phenanthroline) on mixed dithiocarbamate complexes of zinc (II), we report herein, the synthesis, characterization and biological evaluation of 2, 2'-bipyridine, 1, 10-phenanthroline and pyridine adducts of Zinc (II) mixed ligand complex of *N*-methyl-*N*-phenyl dithiocarbamate (L^1) and *N*-ethyl-*N*-phenyl dithiocarbamate (L^2).

2. Experimental

2.1. General

All reagents and solvents were commercially available high grade materials (Merck/Sigma Aldrich) and were used as received. The solvents were purified by standard methods [19].

2.2. Physical measurements

Elemental analysis was performed on an Elementar, Vario EL Cube, set up for CHNS analysis. Infrared spectra were recorded on a Bruker alpha-P FT-IR spectrometer in the frequency range 4000 – 500 cm^{-1} . The NMR spectra were recorded on a 600 MHz Bruker Avance III

NMR spectrometers at room temperature in CDCl_3 . The electronic spectra of the metal complexes were recorded on a Perkin-Elmer $\lambda 20$ UV-VIS spectrophotometer in chloroform. Room temperature magnetic moments and molar conductance measurements were recorded on Sherwood susceptibility balance MSB Mark 1 and Hanna conductivity model H19991300 meters respectively.

2.3. Chemistry

2.3.1. Synthesis of ligands and precursor complex $[\text{ZnL}^1\text{L}^2]$

The ligands, ammonium *N*-methyl-*N*-phenyl dithiocarbamate and ammonium *N*-ethyl-*N*-phenyl dithiocarbamate, were prepared according to a previously described method with slight modification [20]. Briefly, the respective aniline (0.05 mol) was introduced into a round bottom flask containing cold 15 mL ammonia solution (0.05 mol) placed inside an ice bath. After stirring for 5 min, 3 mL carbon disulphide, CS_2 , (0.05 mol) was added to the mixture. The mixture was stirred for 5 - 6 h and filtered by suction. The precipitate obtained was rinsed with ice-cold ethanol and stored under a very low temperature. The precursor complex was prepared as reported earlier [21]. In brief, a 20 mL aqueous solution of freshly prepared ammonium *N*-methyl-*N*-phenyldithiocarbamate (1.00 g, 0.005 mol) was added to a 20 mL aqueous solution of ammonium *N*-ethyl-*N*-phenyldithiocarbamate (1.07 g, 0.005 mol). The solution was stirred for approximately 2 min. Then, ZnCl_2 (2.22 g, 0.005 mol) dissolved in 20 mL water was added to the mixture and stirred for 1 h. The solid product obtained was rinsed thrice with 30 mL distilled water.

2.3.2. Synthesis of (2, 2'-bipyridyl)(*N*, *N*-methyl phenyl-*N*, *N*-ethyl phenyl dithiocarbamato)zinc(II) [$\text{ZnL}^1\text{L}^2\text{bpy}$]

A 15 mL hot chloroform solution of [ZnL^1L^2] (0.44 g, 0.001 mol) was added into a round-bottom flask containing 20 mL hot ethanol solution of 2,2'-bipyridine (0.156 g, 0.001 mol). The resulting yellow solution was refluxed for 1 h, then concentrated to about 15 mL and filtered. The pale yellow solids which separated out from the solution were filtered after 24 h and dried in the desiccator. Single crystals suitable for X-ray analysis were obtained from slow evaporation of dichloromethane-methanol solvent mixture. (Yield: 0.52 g, 87%; Anal. Calc. for $\text{C}_{27}\text{H}_{26}\text{N}_4\text{S}_4\text{Zn}$ (600.16): C, 54.03; H, 4.37; N, 9.34; S, 21.37. Found: C, 54.12; H, 4.32; N, 9.51; S, 21.35%

2.3.3. Synthesis of (1, 10-phenanthroline)(*N*, *N*-methyl phenyl-*N*, *N*-ethyl phenyl dithiocarbamato)zinc(II) [$\text{ZnL}^1\text{L}^2\text{phen}$]

The procedure for the synthesis of [$\text{ZnL}^1\text{L}^2\text{phen}$] is the same as [$\text{ZnL}^1\text{L}^2\text{bpy}$] except that chloroform was used in place of ethanol. A 15 mL hot chloroform solution of 1,10 phenanthroline (0.2 g, 0.001 mol) was added into a hot 35 mL chloroform solution of [ZnL^1L^2] (0.44 g, 0.001 g). The mixture was refluxed for 1 h, then concentrated to about 20 mL. The pale yellow solids which separated out from the solution were filtered after 24 h and dried in a desiccator. (Yield: 0.45 g, 72%; Anal. Calc. for $\text{C}_{29}\text{H}_{26}\text{N}_4\text{S}_4\text{Zn}$ (624.18): C, 55.80; H, 4.19; N, 8.98; S, 20.55. Found: C, 55.75; H, 4.22; N, 8.98; S, 20.54%

2.3.4. Synthesis of (pyridyl)(*N*, *N*-methyl phenyl-*N*, *N*-ethyl phenyl dithiocarbamato)zinc(II) [$\text{ZnL}^1\text{L}^2_2\text{py}$].

The adduct [$\text{ZnL}^1\text{L}^2\text{py}$] was prepared following an earlier reported method [22]. About 0.4 g [ZnL^1L^2] was dissolved in 20 mL pyridine solution, and the solution was refluxed for 3 h at a temperature between 80 and 85 °C. The reaction gave a clear solution, and shortly afterwards some white precipitate began to form. After the reaction, the pyridine solution was filtered off and the precipitates obtained were rinsed with water followed by ethanol and recrystallized from hot chloroform. (Yield: 0.174 g, 75%; Anal. Calc. for $\text{C}_{22}\text{H}_{23}\text{N}_3\text{S}_4\text{Zn}$ (523.08): C, 50.52; H, 4.43; N, 8.03; S, 24.52. Found: C, 51.01; H, 4.42; N, 8.10; S, 22.42%.

2.4. X-ray crystallography

Diffraction data for [$\text{ZnL}^1\text{L}^2\text{bpy}$] was recorded at 200 K using a Bruker Kappa Apex II diffractometer with graphite monochromated Mo $\text{K}\alpha$ radiation ($\lambda = 0.71073 \text{ \AA}$). APEXII was used for data collection and SAINT for cell refinement and data reduction [23]. The structures were solved by direct methods using SHELXS-2014 [24], and refined by least-squares procedures using SHELXL-2014 [25] with SHELXLE [26] as a graphical interface. All non-hydrogen atoms were refined anisotropically, and the hydrogen atoms were calculated in idealized geometrical positions. The H atoms of the alkyl groups were allowed to rotate with a fixed angle around the C–C bond to best fit the experimental electron density (HFIX 137 in the SHELX program suite [25], with Uiso(H) set to 1.5Ueq(C). Data were corrected for absorption effects by the numerical methods using SADABS [23]. Reflections obscured by the beam stop were omitted from the refinement.

2.5. Antimicrobial studies

Antibacterial and antifungal activities were carried out using disc diffusion method [26]. Petri plates were prepared with 20 mL of sterile Mueller–Hinton agar (MHA). The test cultures were swabbed on the top of the solidified media and allowed to dry for 15 min. Specific amount (25 μ L from the 500 μ g/mL) of the compound was introduced into each disc. The loaded discs were placed on the surface of the medium and left for 30 min at room temperature for compound diffusion. Negative control was DMSO. The plates were incubated for 24 h at 37 °C for bacteria and for 48 h at 30 °C for fungi. Zones of inhibition were recorded in millimetres and the experiment was repeated twice. The bacteria strains were *Escherichia coli*, *Klebsilla oxytoca*, *Bacillus cereus*, *Psuedomonas aureginosa*, *salmonila typhi* and *Staphylococcus aureus*. While the fungi organisms were *Aspergillus flavus* and *Fasiparium oxysporium*.

2.5.1. Minimum inhibitory concentration (MIC)

Minimum inhibitory concentration studies of the complexes were performed according to the standard method for bacteria [26] and fungi [27]. Different concentrations (200, 100, 50 and 10 μ g/mL) of the compounds were dissolved in DMSO (2 %) and used. They were added to each medium in 96-well plates. An inoculum of 100 μ L from each well was inoculated. Fluconazole as an antifungal agent and Streptomycin as antibacterial agent were included in the assays as positive controls. For fungi, the plates were incubated for 48 – 72 h at 30 °C and 24 h at 37 °C for the bacteria. The MIC for fungi was defined as the lowest sample concentration, showing no visible fungal growth after incubation time. 5 μ L of tested broth was placed on the sterile MHA plates for bacteria and incubated at respective temperature.

The MIC for bacteria was determined as the lowest concentration of the compound inhibiting the visual growth of the test cultures on the agar plate.

3. Results and Discussion

3.1. Synthesis

The reactions of mixed ligand complex of Zn(II) containing different *N*-alkyl-*N*-phenyl dithiocarbamate with 2,2'-bipyridine, 1,10-phenanthroline, and pyridine at elevated temperature afforded four monomeric adducts. The reaction involving 2,2'-bipyridine and 1,10-phenanthroline were conducted in chloroform/ethanol solvent media, but in the reaction involving the pyridine, the pyridine acted both as the Lewis base and also the solvent medium. During the reaction, the precursor complex first dissolved in the solvent and the central metal utilises its outer d-orbital to form an adduct with the N-donor ligands [22]. While $[ZnL^1L^2bpy]$ and $[ZnL^1L^2phen]$ appeared as bright yellow solution, the $[ZnL^1L^2py]$ precipitated out from the pyridine as a white product upon the adduct formation. All the compounds are soluble in dichloromethane, tetrahydrofuran, and DMSO. The schematic representation of the reaction routes are presented in scheme 1.

3.2. FTIR studies

In general, the IR spectra of dithiocarbamate compounds show three main regions of interest: the region primarily associated with $\nu(C-N)$ of NCS_2 which appears in the range of $1580 - 1450\text{ cm}^{-1}$, the $1060 - 940\text{ cm}^{-1}$ region which is attributed to the asymmetric $\nu(C-S)$ of CSS , and the $420 - 250\text{ cm}^{-1}$ region which is assigned to $\nu(M-S)$ bond [28-30]. The

thioureide peaks were observed in the region of 1454 – 1490 cm^{-1} . The position of the bands indicates a partial double bond character in the CN bond of $\text{S}_2\text{C}-\text{NR}_2$. The stretching frequencies of single (C–N) bond appears in the range 1250 – 1360 cm^{-1} , while doubly bonded carbon and nitrogen (C=N) is expected around 1640 – 1690 cm^{-1} [31]. The single and strong peaks at 969 – 984 cm^{-1} are attributed to C=S stretch of a symmetrically bound dithiocarbamate [32]. The spectra of $[\text{ZnL}^1\text{L}^2\text{bpy}]$ showed two other peaks at 1025 and 1007 cm^{-1} in addition to the observed peak at 969 cm^{-1} . This indicates the presence of two different binding fashion. The occurrence of a single peak is indicative of bidentate coordination of the dithio ligand, while for a monodentate unsymmetrically coordination of the ligand to the central metal, a doublet is observed [32].

3.3. NMR studies

3.3.1. ^1H -NMR

The ^1H -NMR chemical shifts (ppm) of the complexes are presented in Table 1. All the complexes displayed peaks in the range 7.49 – 7.34 ppm and 7.33 – 7.14 ppm, which are ascribed to the aromatic rings from the *N*-ethyl-*N*-phenyl dithiocarbamate and *N*-methyl-*N*-phenyl dithiocarbamate groups respectively. The methyl group and the methylene group of the ethyl substituents resonated between 1.18 – 1.27 ppm as triplet, and between 4.18 – 4.24 ppm as quartet respectively in all the complexes. A sharp singlet observed around 3.67 – 3.75 ppm is ascribed to the methyl group linked directly to the N atoms contained in the dithiocarbamate moiety, while the peaks due to the protons of the pyridine molecule in $[\text{ZnL}^1\text{L}^2\text{py}]$ appeared between 9.00 – 7.48 ppm. The downfield shift of the peaks associated with the protons of the ethyl and methyl groups in these compounds relative to position of

the protons of allylic methyl and ethyl (1.7 ppm) could be due to the effect of the electronegativity of the aromatic groups, and also the relative proximity of the alkyl substituents to the thioureide bond and metal center [22]. The signals due to the 2, 2'-bipyridine and 1,10-phenanthroline appeared at 9.09, 8.07, 7.95, 7.83 ppm and at 9.62, 9.52, 8.47, 8.33, 7.82 ppm respectively.

3.3.2. ^{13}C -NMR

Table 2 contains the ^{13}C -NMR chemical shifts (ppm) of the complexes. The complexes exhibit a low field resonance which is associated with the backbone carbon of the dithiocarbamate [33]. Two distinct peaks were observed at approximately 207.0 and 209.0 ppm. The occurrence of two NCS_2 peaks is the consequence of different alkyl substituents (methyl/ethyl) on the magnetic equivalence of the two groups of dithiocarbamate. The ligating group (dithiocarbamate) with higher electronic density would have a more shielded $-\text{CS}_2$ carbon [34]. While the methylene carbon of the ethyl group resonated between 53.0 – 56.0 ppm and the methyl carbon of the pyridine appeared between 46.0 to 47.0 ppm, the methyl group of the ethyl substituent was observed at the upfield region between 12.35 to 12.62 ppm. This relatively low resonant frequency is attributed to the distance of the methyl groups from the deshielding influence of the electronegative nitrogen and the thioureide π -system [35, 36]. In the aromatic region, signals due to the pyridine molecule of $[\text{ZnL}^1\text{L}^2\text{py}]$ occurred at 149.32, 138.83, and 124.83. The signals due to the carbon atoms of the phenyl rings appeared between 147.0 to 125.0 ppm. In the Table, these signals have been grouped into two: peaks due to the aromatic carbons of the *N*-ethyl unit and peaks due to the *N*-

methyl unit. The occurrence of these peaks in different environments is an indication of the magnetic un-equivalence of the aromatic groups [37].

3.4. Electronic spectra, magnetic susceptibility and conductance measurement

The electronic spectra showed bands at 225 nm, 275 nm, 355 nm, 430 nm ($\epsilon = 10890 \text{ m}^2\text{mol}^{-1}$) for $[\text{ZnL}^1\text{L}^2\text{bpy}]$; 210 nm, 270 nm, 300 nm, 410 nm ($\epsilon = 10243 \text{ m}^2\text{mol}^{-1}$) for $[\text{ZnL}^1\text{L}^2\text{phen}]$ and 205 nm, 255 nm, 290 nm, 325 nm, 520 nm ($\epsilon = 12678 \text{ m}^2\text{mol}^{-1}$) for $[\text{ZnL}^1\text{L}^2\text{py}]$. The bands around 205 – 290 nm are intra-ligand bands due to $n - \pi^*$ transition and those bands around 290 – 355 nm are also intra-ligand bands due to $\pi - \pi^*$ transitions. For d^{10} complexes, no d-d transitions are expected, however, bands observed in the visible region of the complexes are metal to ligand charge transfer (MLCT) bands consistent of a d^{10} system that tailed into the visible region. These results are in agreement with reported values [7, 38, 39].

Zinc complexes are diamagnetic, thus give a sub-zero magnetic moment [40]. The magnetic susceptibility values for $[\text{ZnL}^1\text{L}^2\text{phen}]$, $[\text{ZnL}^1\text{L}^2\text{bpy}]$, $[\text{ZnL}^1\text{L}^2\text{py}]$ and $[\text{ZnL}^1\text{L}^2]$ are 0.42 BM, 0.32 BM, 0.28 BM and 0.23 BM respectively, and are similar to reported data obtained from similar complexes [38, 39]. The metal(II) complexes are non-electrolytes in nitromethane as shown by their molar conductivities that are between $32 - 50 \text{ ohm}^{-1}\text{cm}^2\text{mol}^{-1}$, which are lower than reported value of $60 - 118 \text{ ohm}^{-1}\text{cm}^2\text{mol}^{-1}$ for a 1:1 electrolyte [41].

3.5. Description of crystal structures

Details of crystal data and structure refinements are provided in Table 3. Selected bond lengths and bond angles are shown in Tables 4. The molecular structure of the complex is shown in Figure 1 while the packing diagram is shown in Figure 2. The structure consists of mononuclear species in which the central zinc atom is surrounded by two dithiocarbamate ligands and one bipyridine molecule. The two dithiocarbamate ligands are disordered in 0.67:0.33 ratio and alternatively bond as monodentate (Figure 1a) and bidentate ligands (Figure 1b). In the minor disorder state the ligand that was monodentate becomes bidentate, while the bidentate ligand becomes monodentate. So in both cases only three out of the four Sulphur atoms of the two dithiocarbamates are coordinated to the zinc atom. Therefore, at one time in both disordered states there is one long Zn-S distance showing that there is always one dithiocarbamate ligand that is bidentate, and one monodentate. To further highlight this, major disorder component (0.666) and minor disorder component (0.334) have been presented in Table 5. The bipyridine acts as a bidentate ligand and gives the structure around the Zn atom a distorted square pyramidal geometry. τ value, which can determine how closely a distorted compound approximates either a trigonal bipyramidal (tbp) or square pyramidal (sqp) geometry, was calculated using the formula $\tau = (\beta - \alpha)/60$, where $\alpha(c - e)$ and $\beta(b - d)$ are the angles that are opposite each other in the xy plane [42]. The τ value was obtained as 0.28 and corroborates a distorted sqp geometry. In a similar reported Zn(II) [43] and Cd(II) [44] adducts involving dithiocarbamate (homoleptic) and 2,2-bipyridine, monodentate fashion of bonding was observed in the Zn complex while both dithiocarbamate exhibited a bidentate coordination in the Cd complex. It is possible that, the Cd atom was able to accommodate all the ligating atoms due to its larger size. However, while distorted trigonal pyramidal structure was

reported for the zinc complex, the cadmium atom existed in a highly distorted octahedral environment. In both complexes [43, 44] no disorder was observed in the alkyl groups apparently because both dithiocarbamate units contains similar alkyl groups. In the present study, the distortion from the regular square pyramidal geometry of $[\text{ZnL}^1\text{L}^2\text{bpy}]$ may be due to the small bite angle of the chelating ligands- dithiocarbamate: $\text{S}(21)\text{--Zn}(1)\text{--S}(22)$, $\text{S}(33)\text{--Zn}(1)\text{--S}(34)$ and bipyridine: $\text{N}(11)\text{--Zn}(1)\text{--N}(12)$, whose chelate angles ($70.99(5)$, $72.23(9)$ and $74.86(7)^\circ$), respectively deviate significantly from the expected 90° . The dithiocarbamate ligands have a dihedral angle of $58.70(0.10)^\circ$ and $61.61(0.06)^\circ$ with the bipyridine ligand. The methyl and ethyl groups are alternatively disordered on the two dithiocarbamate ligands in a 0.51:0.49 ratio. There are a number of C—H...S interactions linking the complexes in the unit cell.

3.6. Antimicrobial studies

The complexes were assessed for their antimicrobial activity against six bacteria strains and two fungi organisms at a concentration of $100\ \mu\text{g}/\text{mL}$ (Table 6, Figure 3). The complexes showed moderate to good antimicrobial activity against the Gram negative and Gram positive bacteria strains and fungi organisms. On structure activity relationship, the $[\text{ZnL}^1\text{L}^2]$ complexes had the best activity against both bacteria and fungi organisms. The antimicrobial activities of the complexes were in the order of $[\text{ZnL}^1\text{L}^2] > [\text{ZnL}^1\text{L}^2\text{py}] > [\text{ZnL}^1\text{L}^2\text{bpy}] > [\text{ZnL}^1\text{L}^2\text{phen}]$.

In most cases, the mechanism of antimicrobial action of metal complexes has been attributed to the degree of lipophilicity of the complexes through the microbial cell wall. The

variation in the effectiveness of different compounds against different organisms depends either on the impermeability of the cells of the microbes or on differences in ribosome of microbial cells [45]. The size of a complex could be considered a factor that affects its Permeability through the microbial cell wall [46]. Arranging the complexes in order of increasing molecular weight gives $[\text{ZnL}^1\text{L}^2] < [\text{ZnL}^1\text{L}^2\text{py}] < [\text{ZnL}^1\text{L}^2\text{bpy}] < [\text{ZnL}^1\text{L}^2\text{phen}]$, which is in agreement with the order of decreasing antimicrobial activity. Although, the exact mechanism of antimicrobial activity of our complexes is not fully understood biochemically, mode of action of antimicrobial agents may include any of the following mechanism: (i) Interference with the cell wall synthesis, damage as a result of which cell permeability may be altered (or) they may disorganize the lipoprotein leading to the cell death. (ii) Deactivate various cellular enzymes, which play a vital role in different metabolic pathways of these microorganisms. (iii) Denaturation of one or more proteins of the cell, as a result of which the normal cellular processes are impaired. (iv) Formation of hydrogen bond between the donor group and the active center of cell constituents, resulting in interference with the normal cell process [47].

The minimum inhibitory concentration of the complexes is presented in Table 7, and it shows the lowest concentration of the complexes at which antimicrobial activity were visible. This was achieved through serial dilution of the stock solution of the complex to various concentrations of 75 $\mu\text{g}/\text{mL}$, 50 $\mu\text{g}/\text{mL}$ and 25 $\mu\text{g}/\text{mL}$. $[\text{ZnL}^1\text{L}^2]$ showed the lowest MIC of the test complexes at 25 $\mu\text{g}/\text{mL}$ and, as such, considered as the complex with most antimicrobial activity against the selected microorganisms. Generally, the precursor complex, $[\text{ZnL}^1\text{L}^2]$, showed greater antibacterial activity compared to streptomycin against S.

aureus, B. cerus, K. oxytoca and E. coli. Similarly $[\text{ZnL}^1\text{L}^2\text{py}]$ exhibited greater antibacterial activity against S. aureus and K. oxytoca. The compounds showed higher antibacterial activity compared to the positive control against some of the microbes.

Conclusion

We synthesized new heteroleptic complexes by the reaction of mixed ligands dithiocarbamates complex of zinc with different Lewis bases (pyridine, 2, 2 bipyridine, and 1, 10-phenanthroline), with a view of evaluating the antimicrobial properties of these compounds and relating them to the change in the size of the compounds with respect to the precursor complex. The synthesized compounds were characterized by elemental analysis and spectroscopic techniques. The 2,2 bipyridine adducts which was further characterized by single crystal X-ray diffraction indicated that the Zn atom is in a distorted square pyramidal geometry, and the methyl and ethyl groups are alternatively disordered on the two dithiocarbamate ligands. The antimicrobial activities of the complexes were in the order $[\text{ZnL}^1\text{L}^2] > [\text{ZnL}^1\text{L}^2\text{py}] > [\text{ZnL}^1\text{L}^2\text{bpy}] > [\text{ZnL}^1\text{L}^2\text{phen}]$. The lowest MIC was exhibited by $[\text{ZnL}^1\text{L}^2]$ which is considered as the complex with most antimicrobial activity against the selected microorganisms.

Supplementary material

CCDC 1452156 contains the supplementary crystallographic data for this paper. These data can be obtained free of charge from The Cambridge Crystallographic Data Centre via

www.ccdc.cam.ac.uk/data_request/cif or from the Cambridge Crystallographic Data Centre,
12 Union Road, Cambridge CB2 1EZ, UK; fax: (+44) 1223 336 033; or e mail:
deposit@ccdc.cam.ac.uk.

References

- [1] T. G. Spiro, Ed. Zinc Enzymes, Wiley: New York, 1983.
- [2] J.M. Berg, Science, Washington, D.C. 232 (1986) 485.
- [3] S. Bhattacharyya, S.B. Kumar, S.K. Dutta, R.T.T. Edward, M. Chaudhury, Inorg. Chem. 35 (1996) 1967.
- [4] R.J.P. Williams, Pure Appl. Chem. 54 (1982) 1889.
- [5] H.A. Tajmir-Riahi, M. Langlais, R. Savoie, Nucleic Acids Res. 16 (1988) 751.
- [6] C. Orvig, M.J. Abrams, Chem. Rev. 99 (1999) 2201.
- [7] P.J. Rani, S. Thirumaran, S. Ciattini, Spectrochim. Acta 137A (2015) 1164.
- [8] A.C. Ekennia, D.C. Onwudiwe, A.A. Osowole, J. Sulfur Chem. 36 (2015) 96.
- [9] D.C. Onwudiwe, P.A. Ajibade, Inter. J. Mol. Scien.12 (2011) 1964.
- [10] W. H. Tisdale, I. Williams, Disinfectant, US197296, 1934.
- [11] O.H.J. Szolar, Anal. Chim. Acta 582 (2007) 191.
- [12] L. Nand, Chem. Biol. Interf. 4 (2014) 321.
- [13] B. K. Shashi, K. Geetanjli, Priyanka, Himachal Pradesh Univ. J. 1 (2011) 1.
- [14] A.C. Ekennia, D. C. Onwudiwe, C.Ume, E.E. Ebenso, Bioinorg. Chem. Appl. 2015 (2015) 1
- [15] B.A. Prakasam, K. Ramalingam, G. Bocelli, Phosphorus, Sulfur Silicon Relat. Elem. 184 (2009) 2020.

- [16] A.L. Doadrio, J. Sotelo, A. Fern'andez-Ruano, *Quimica Nova* 25 (2002) 525.
- [17] D. Coucouvanis, J. P. Fackler Jr., *Inorg. Chem.* 6 (1967) 2047.
- [18] G. Hogarth, Transition metal dithiocarbamates: 1978–2003, *Prog. Inorg. Chem.* 53 (2005) 71.
- [19] D.D. Perrin, W.L.F. Armarego, *Purification of Laboratory Chemicals*, 3rd ed., Pergamon: Oxford, 1980.
- [20] D.C. Onwudiwe, P. A. Ajibade, *Polyhedron* 29 (2010) 1431.
- [21] P.A. Ajibade, D.C. Onwudiwe, M.J. Moloto, *Polyhedron* 30 (2011) 246.
- [22] D.C. Onwudiwe, C.A. Strydom, E.C. Hosten, *Inorg. Chim. Acta* 401 (2013) 1.
- [23] APEX2, SADABS and SAINT, Bruker AXS Inc., Madison, Wisconsin, USA, 2010.
- [24] C.B. Hübschle, G.M. Sheldrick, B. Dittrich, *J. Appl. Cryst.* 44. (2011) 1281
- [25] G. M. Sheldrick, *Acta Cryst.* A64 (2008) 112.
- [26] R. Pastorek, J. Kameníček, F. Březina, Z. Šindelář, E. Jehlářová, N.V. Duffy, C.T. Glowiak, *Chem. Papers* 48 (1994) 317.
- [27] C.A. Tsipis, D.P. Kessissoglou, G. A. Katsoulos, *Chim. Chron.* 14 (1985) 195.
- [28] N.H. Abdullah, Z. Zainal, S. Silong, M.I.M. Tahir, K-B. Tan, S-K. Chang, *Mater. Chem. Phys.* xxx (2016) 1-9
- [29] M. Shahid, T. Ruffer, H. Lang, S.A. Awan, S. Ahmad, *J. Coord. Chem.* 62 (2009) 440.
- [30] S. Thirumaran, K. Ramalingam, *Transit. Metal. Chem.* 25 (2000) 60.
- [31] R.R. Martinez, R.M. Huicochea, J.A.G. Alvarez, H. Hopfl, H. Tlahuext. *Ark. V.* (2008) 19.
- [32] F. Bonati, U. Renato. *J. Organomet. Chem.* 10 (1967) 257.

- [33] G. Hogarth, C. Ebony-Jewel, R.C.R. Rainford-Brent, S.E. Kabir, I. Richards, J.D.E.T. Wilton-Ely, Q. Zhang, *Inorg. Chim. Acta.* 362 (2009) 2021.
- [34] S.P. Sovilj, G. Vukovi, K. Babic, T.J. Sabo, S. Macura, N. Juranic, *J. Coord. Chem.* 41 (1997) 25.
- [35] B.A. Prakasam, K. Ramalingam, G. Bocelli, A. Cantoni, *Polyhedron* 26 (2007) 4491.
- [36] R.J. Anderson, D.J. Bendell, P.W. Groundwater, *Organic Spectroscopic Analysis*, RSC, Cambridge, 2004.
- [37] M. Grenier-Loustalot, L. Da Cunha, *Eur. Polym. J.* 34 (1998) 98.
- [38] J.M. Ashurov, A.B. Ibragimov, B.T. Ibragimov, *Polyhedron* 102 (2015) 441.
- [39] S. Thirumaran, K. Ramalingam, G. Bocelli, A. Cantoni, *Polyhedron*, 18 (1999) 925.
- [40] A. Earnshaw, *The Introduction to Magnetochemistry*, Academic Press, London, 1980.
- [41] W.J. Geary, *Coord. Chem. Rev.*, 7(1971) 81.
- [42] M-A. Munoz-Hernandez, T. S. Keizer, P. Wei, S. Parkin, D.A. Atwood, *Inorg. Chem.* 40 (2001) 6782.
- [43] D.C. Onwudiwe, P.A. Ajibade, B. Omondi, *J. Mol. Struct.* 987 (2011) 58.
- [44] P.A. Ajibade, D.C. Onwudiwe. *J. Mol. Struct.* 1034 (2013) 249.
- [45] R. Joseyphus, M. Nair, *Mycobiology* 36 (2008) 93.
- [46] P.J. Rani, S. Thirumaran, *Eur. J. Med. Chem.* (2013) 139.
- [47] L. Malhota, S. Kumar, K.S Dhindsa, *Indian J. Chem*, 32A (1993) 457.

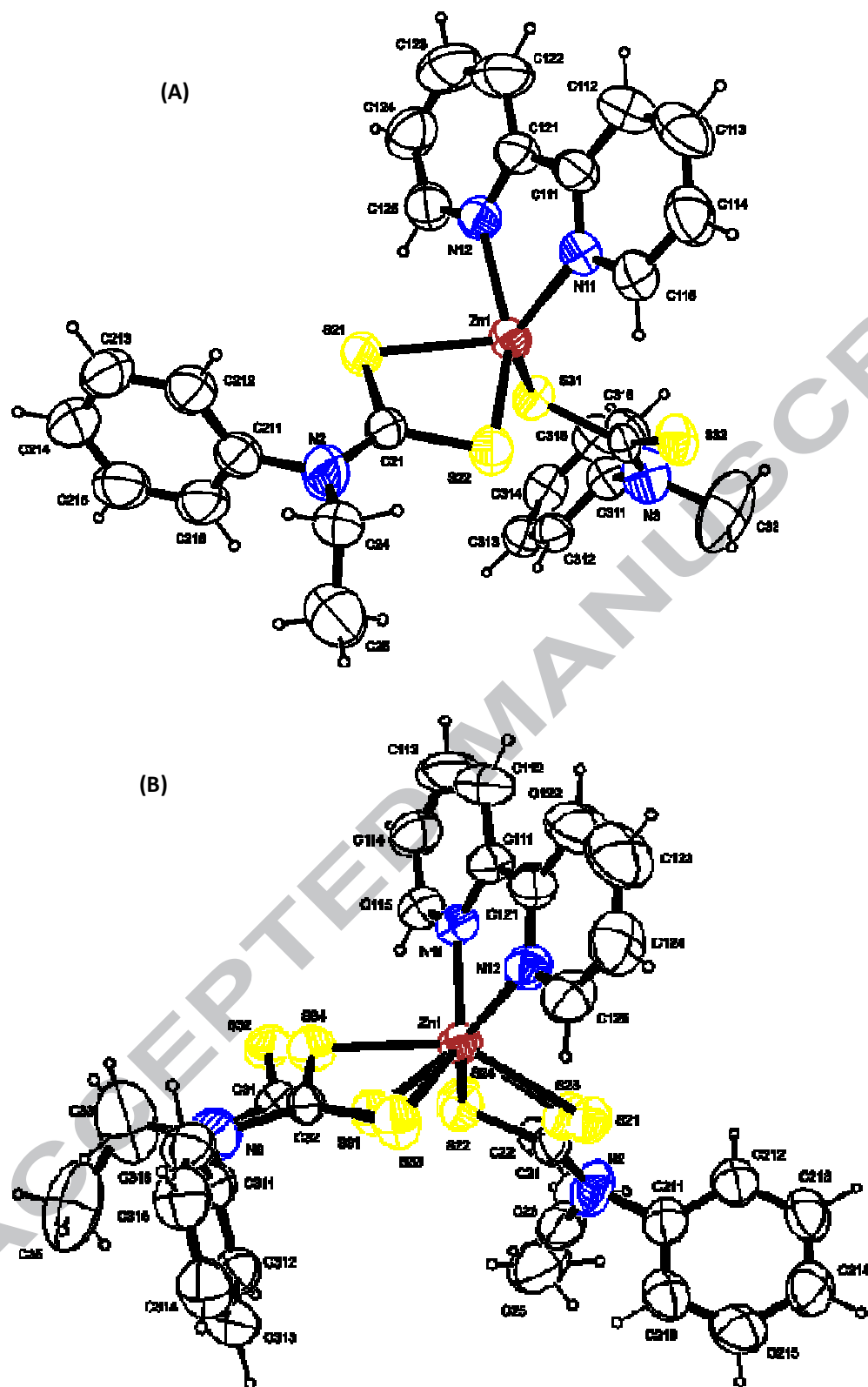


Figure 1: Ortep diagram of $[\text{ZnL}^2\text{bpy}]$ showing (a) monodentate and (b) bidentate fashion of the dithiocarbamate with only the major disordered components shown. Thermal ellipsoids are drawn at 50% probability level.

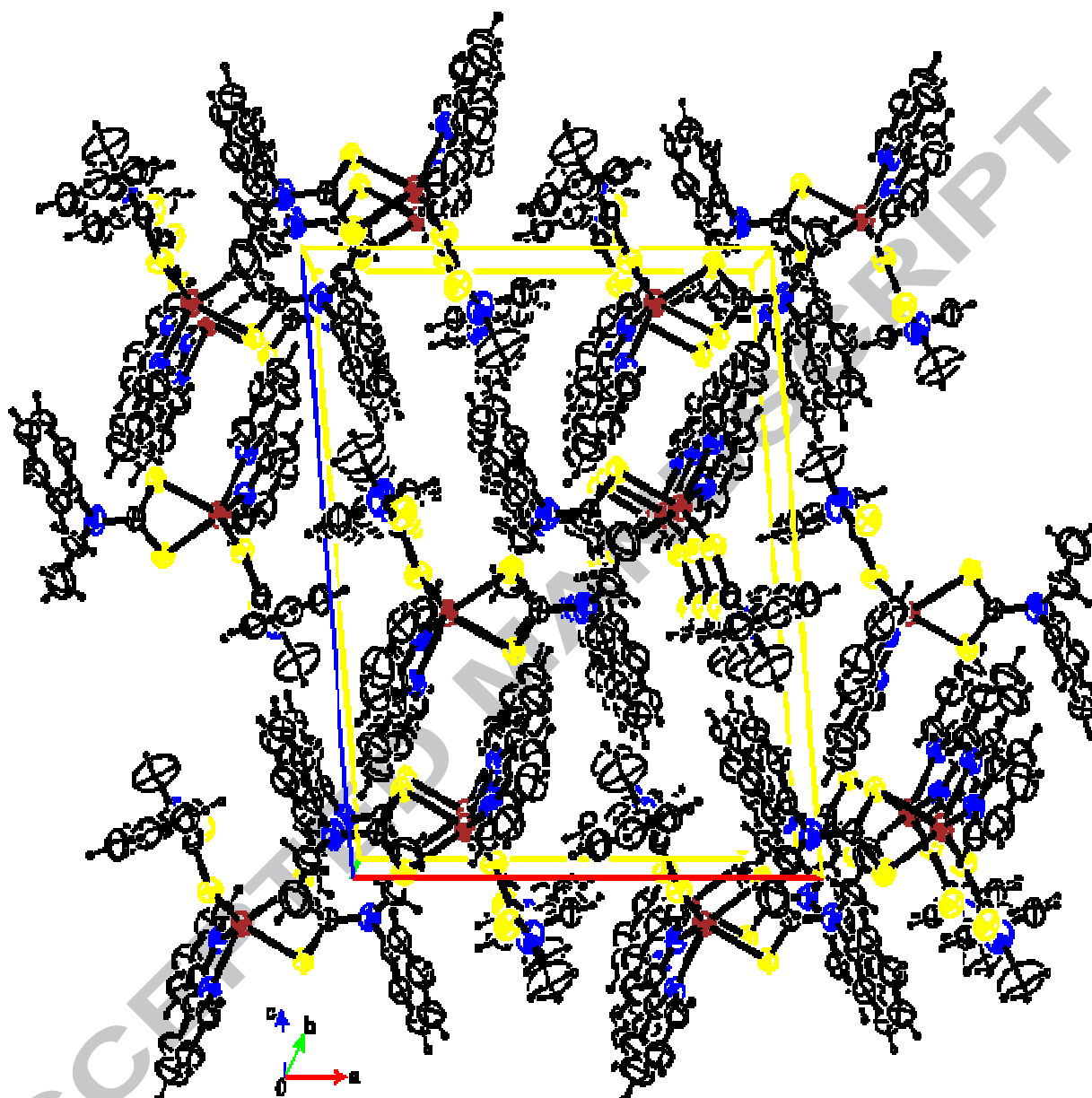


Figure 2: Packing diagram of [ZnL¹L²bpy] viewed normal to (010). Only the major disorder components are shown. Thermal ellipsoids are drawn at 50% probability level.

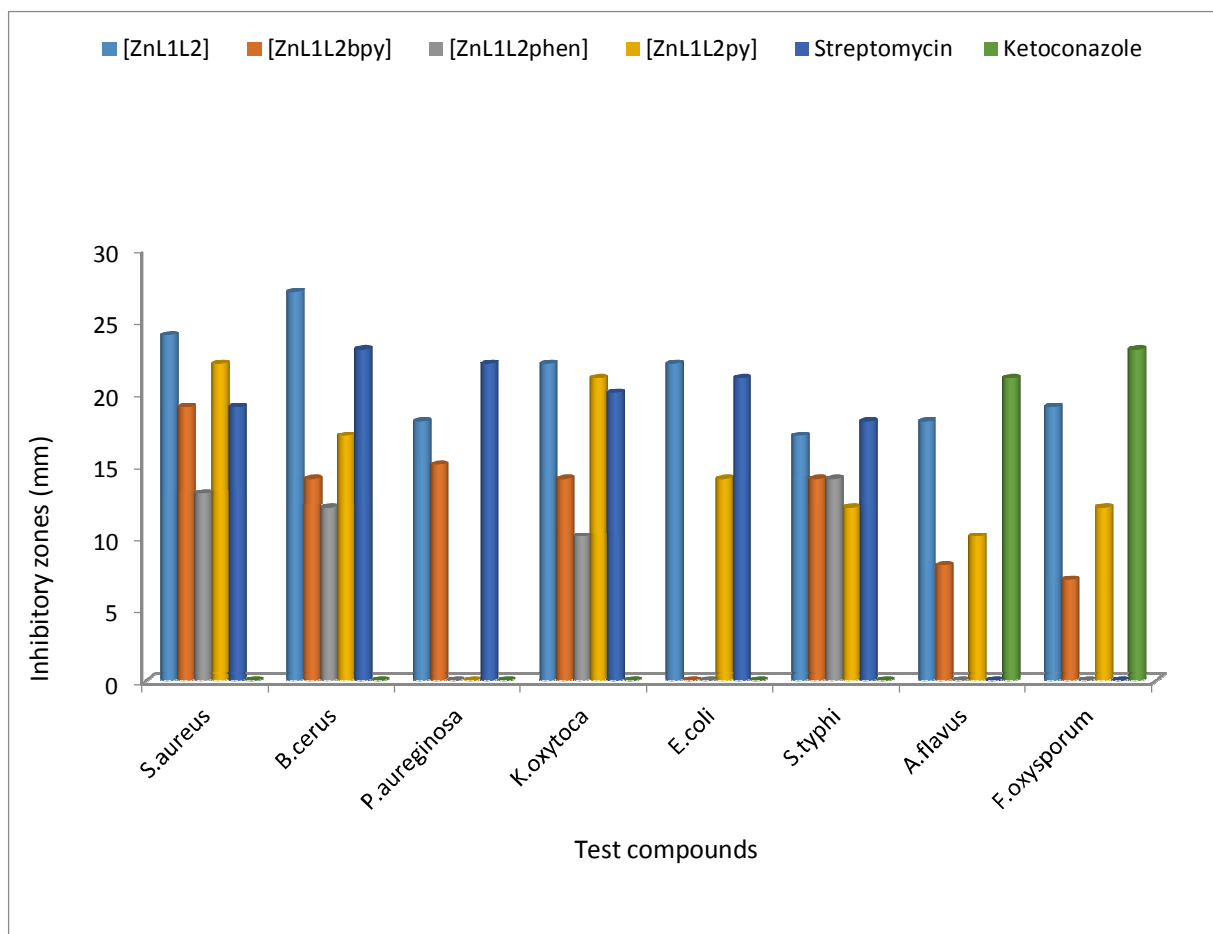


Figure 3: A histogram representation of the antimicrobial data of the complexes

Table 1: $^1\text{H-NMR}$ chemical shifts (ppm) of the complexes

Compound	$\text{C}_6\text{H}_5\text{-}$ N(Et)	$\text{C}_6\text{H}_5\text{-}$ N(Me)	$\text{CH}_3\text{CH}_2\text{-}$ N(C_6H_5)	$\text{CH}_3\text{CH}_2\text{-}$ N(C_6H_5)	$\text{CH}_3\text{-}$ N(C_6H_5)	py	bpy	phen
[ZnL ¹ L ² py]	7.43 – 7.34(m)	7.30- 7.16 (m)	4.18 (q)	1.26 (t)	3.72 (s)	9.00(d) 7.87(t) 7.48(t)	-	-
[Zn L ¹ L ² bpy]	7.49 – 7.36(m)	7.34 – 7.14(m)	4.19 (q)	1.18(t)	3.67(s)	-	9.09(d) 8.07(d) 7.95(q) 7.83(q)	-
[Zn L ¹ L ² phen]	7.41 – 7.35(m)	7.30 – 7.15(m)	4.24(q)	1.23	3.75(s)	-	-	9.62(s) 9.52(s) 8.47(d) 8.33(d) 7.82(d)

Table 2: ^{13}C -NMR chemical shifts (ppm) of complexes

Compound	C_6H_5- N(Et)	C_6H_5- N(Me)	CH_3CH_2- N(C ₆ H ₅)	CH_3- N(C ₆ H ₅)	CS ₂	Py	bpy	phen
	146.73	129.89				149.32		
[ZnL ¹ L ² py]	144.58	128.27	53.86(CH ₂)	46.94	207.96	138.83	-	-
	129.36	127.42	12.38(CH ₃)		207.06	124.83		
		126.82						
	147.77	129.79					150.59	
	145.46	127.45	53.73(CH ₂)	47.07	209.40	-	149.11	-
[ZnL ¹ L ² bpy]	129.12	126.34	12.51(CH ₃)		208.37		138.53	
		125.09						149.07
	147.00	129.78	53.62(CH ₂)	47.10	209.04	-	-	148.18
[ZnL ¹ L ² phen]	145.03	127.82	12.62(CH ₃)		207.54			138.71
	129.71	126.74						137.41
		125.13						

Table 3: Summary of crystal data and structure refinement

Identification Code	[ZnL ^{1,2} bpy]
Empirical Formula	C ₂₇ H ₂₆ N ₄ S ₄ Zn
Formula weight	600.15
Crystal System	Monoclinic
Wavelength	0.71073 Å
Crystal system	Monoclinic
Space group	P2 ₁ /n
Unit cell dimensions	
a (Å)	15.5021(9)
b (Å)	9.8197(6)
c (Å)	18.7538(11)
α (°)	90
β (°)	95.021(2)
γ (°)	90
V [Å ³]	2843.9(3)
Z	4
D(calc) (g/cm ³)	1.402
μ(MoKa) (/mm)	1.181
F(000)	1240
Crystal size (mm)	0.18 x 0.41 x 0.42
Temperature (K)	200
Radiation (Å)	0.71073
θ Min-Max (°)	1.8 - 28.3
Dataset	-19:20 ; -13:12 ; -25:24
Tot., Uniq. Data	39253, 7068,
R(int)	0.016
[I > 2.0 sigma(I)]	5561
Nref, Npar	7068, 394
R	0.0356
wR2	0.1007
S	1.05
Max. and Av. Shift/Error	0.00, 0.00
Min. residual density [e/Å ³]	-0.29
Max. residual density [e/Å ³]	0.55

Table 4: Selected bond distances and angles for [ZnL¹L²bpy]

Bond	distances (Å)	Bond	angles (°)
Zn1– S21	2.4573(17)	S21 – Zn1 – S22	70.99(5)
Zn1– S22	2.5753(13)	S21 – Zn1 – S31	108.39(6)
Zn1– S31	2.3166(16)	S21 – Zn1 – N11	118.03(7)
Zn1– S23	2.217(3)	S21 – Zn1 – N12	86.97(6)
Zn1– S33	2.543(3)	S22 – Zn1 – S31	112.81(5)
Zn1– S34	2.424(3)	S22 – Zn1 – N11	95.81(6)
Zn1– N11	2.1014(19)	S22 – Zn1 – N12	148.76(6)
Zn1– N12	2.2336(19)	S31 – Zn1 – N11	131.38(6)
S21– C21	1.694(5)	S31 – Zn1 – N12	94.75(6)
S22– C21	1.702(5)	S23 – Zn1 – S33	106.08(10)
S23– C22	1.719(12)	S23 – Zn1 – S34	135.33(11)
S24– C22	1.691(11)	S23 – Zn1 – N11	115.22(10)
S31– C31	1.732(4)	S23 – Zn1 – N12	98.45(10)
S32– C31	1.692(5)	S33 – Zn1 – S34	72.23(9)
		S33 – Zn1 – N11	135.78(9)
		S33 – Zn1 – N12	84.43(9)
		S34 – Zn1 – N11	88.30(7)
		S34 – Zn1 – N12	125.04(8)
		N11 – Zn1 – N12	74.86(7)

Table 5: Zn—S distances (Å) in the disordered components showing that in both cases only three Zn—S bonds are coordinating at one time.

Major disorder component (0.666)		Minor disorder component (0.334)	
Zn1—S21	2.4573(17)	Zn1—S23	2.217(3)
Zn1—S22	2.5753(13)	Zn1—S24	3.266(3)
Zn1—S31	2.3166(16)	Zn1—S33	2.543(3)
Zn1—S32	3.2094(18)	Zn1—S34	2.424(3)

Table 6: Antimicrobial results of the complexes

Complexes	S.aureus	B.cerus	P.aureginosa	K.oxytoca	E.coli	S.typhi	A.flavus	F.oxysporum
(100 µg/mL)								
[ZnL ¹ L ²]	24±0.7	27±0.0	18±0.7	22±0.0	22±0.7	17±2.1	18±0.7	19±0.0
[ZnL ¹ L ² bpy]	19±0.0	14±2.1	15±2.1	14±2.1	-	14±1.4	08±0.7	07±2.1
[ZnL ¹ L ² phen]	13±0.7	12±0.7	-	10±2.1	-	14±1.4	-	-
[ZnL ¹ L ² py]	22±1.4	17±0.7	-	21±0.7	14±2.1	12±0.7	10±0.7	12±1.4
Streptomycin	19±0.7	23±0.7	22±1.4	20±0.7	21±0.7	18±0.0	NS	NS
Ketoconazole	NS	NS	NS	NS	NS	NS	21±0.7	23±0.0

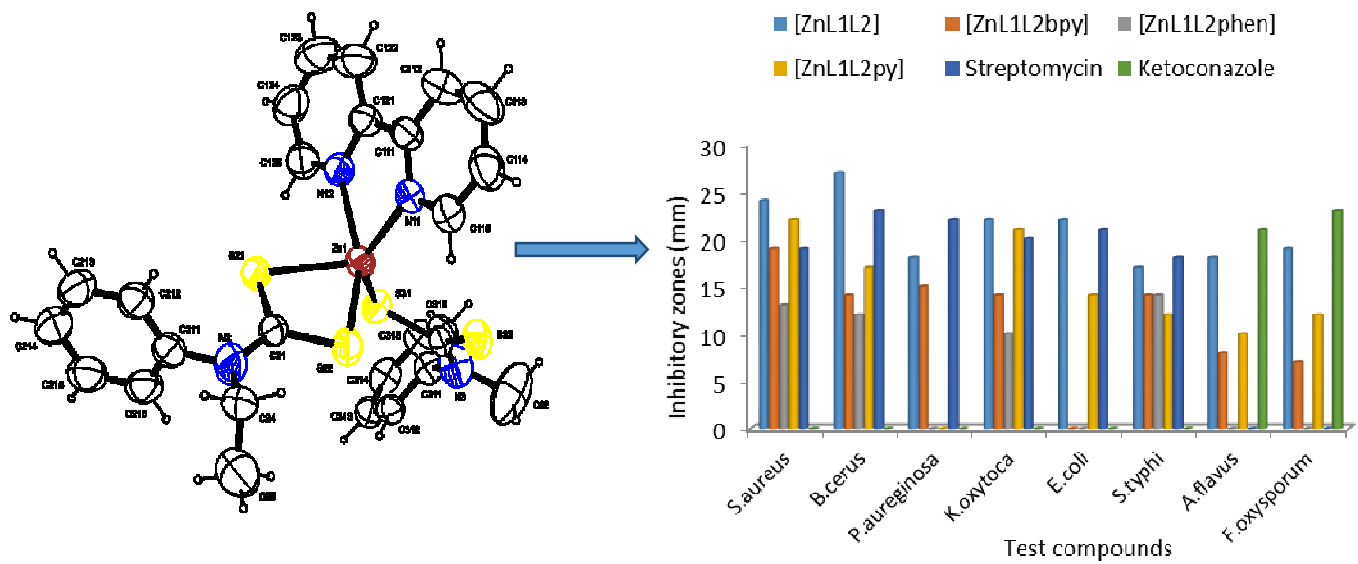
Values (in mm) represent the average of two replications and is standard deviation; Streptomycin (antibiotic) was used as positive control for antibacterial screening, Ketoconazole (antifungal) was used as positive control for antifungal screening, '-' denotes resistant 'NS' denotes not screened.

Table 7: Minimum inhibitory concentration (MIC) of the complexes

Complexes	S.aureus	B.cerus	P.aureginosa	K.oxytoca	E.coli	S.typhi	A.flavus	F.oxysporum
[ZnL ¹ L ²]	50	50	50	25	25	25	50	75
[ZnL ¹ L ² bpy]	75	75	50	75	-	50	75	75
[ZnL ¹ L ² phen]	75	75	-	100	-	100	-	-
[ZnL ¹ L ² py]	50	75	-	100	75	50	50	75
Streptomycin	<25	<25	<25	25	25	<25	NS	NS
Ketoconazole	NS	NS	NS	NS	NS	NS	<25	<25

Values (in µg/mL)

Graphical Abstract



ACCEPTED M.

Graphical abstract

- Ortep diagram of $[\text{ZnL}^1\text{L}^2\text{bpy}]$ with only the major disordered components shown. Thermal ellipsoids are drawn at 50% probability level
- A histogram representation of the antimicrobial data of the synthesised complexes

ACCEPTED MANUSCRIPT

Highlights

- Zn(II) adducts containing different N-donor ligands were synthesized and characterized
- Structure of the bpy adducts show the methyl and ethyl groups are alternatively disordered
- The antimicrobial activities of the complexes were evaluated
- The highest antimicrobial property was exhibited by the precursor complex

ACCEPTED MANUSCRIPT